Molecular Therapy
Oncolytics
Original Article

Collateral Lethal Effects of Complementary Oncolytic Viruses

Justin W. Maroun,[1,2] Velia Penza,[1] Taylor M. Weiskittel,[1,2] Autumn J. Schulze,[1] and Stephen J. Russell[1]

[1]Department of Molecular Medicine, Mayo Clinic College of Medicine, Rochester, MN 55905, USA; [2]Medical Scientist Training Program, Mayo Clinic Alix School of Medicine, Rochester, MN, USA

Virus-infected cells release type 1 interferons, which induce an antiviral state in neighboring cells. Naturally occurring viruses are therefore equipped with stealth replication strategies to limit virus sensing and/or with combat strategies to prevent or reverse the antiviral state. Here we show that oncolytic viruses with simple RNA genomes whose spread was suppressed in tumor cells pretreated with interferon were able to replicate efficiently when the cells were coinfected with a poxvirus known to encode a diversity of innate immune combat proteins. *In vivo* the poxvirus was shown to reverse the intratumoral antiviral state, rescuing RNA virus replication in an otherwise restrictive syngeneic mouse tumor model leading to antitumor efficacy. Pairing of complementary oncolytic viruses is a promising strategy to enhance the antitumor activity of this novel class of anticancer drugs.

INTRODUCTION

Oncolytic virotherapy is emerging as a promising new cancer treatment modality. It has been well demonstrated that oncolytic viruses can target tumors with defects in their innate ability to sense and respond to viral infections.[1–3] In consequence, many of the oncolytic viruses currently in development were attenuated by evolving or adapting them to impair their ability to combat innate immunity such that they are highly sensitive to interferon (IFN)-mediated antiviral restriction.[4] Mounting evidence, however, indicates that there is considerable heterogeneity of innate antiviral immune defenses within and between tumor types.[5] As we and others have demonstrated, many tumor cell lines, as well as primary human tumors, mount robust innate antiviral immune responses. Additionally, although many cell lines prove highly susceptible to oncolytic viruses in culture, growth within a tumor microenvironment populated by stromal elements can lead to the induction of a constitutive antiviral state in tumor cells that are IFN responsive, preventing a spreading oncolytic infection.[6]

Mengovirus, a picornavirus with a small positive sense RNA genome, and vesicular stomatitis virus (VSV), a rhabdovirus with a small negative sense RNA genome, are currently being developed as oncolytic agents.[7,8] Both are highly sensitive to the antiviral actions of IFN.[9] Mengovirus has a broad tissue tropism and a fast and lytic life cycle, but has been attenuated and detargeted via truncation of the polycytidine tract in the 5′ untranslated region from 55 to 24 cytidines (MC_{24}) and insertion of muscle- and neuron-specific microRNA targets into the viral genome ($MC_{24}NC$).[8,10] VSV is currently under clinical development as an oncolytic vector and has been reviewed extensively.[11,12] The VSV used in the current study and clinical trials was attenuated by encoding IFNβ in the genome.[13] Although MC_{24} and VSV are both therapeutically active against certain syngeneic murine tumor models,[8] they are unsurprisingly no exception to the commonly observed discrepancy between *in vitro* susceptibility and *in vivo* efficacy among IFN-responsive tumor cell lines.[6,14,15]

Innate immune signaling in tumor cells can be triggered in a virus-dependent or -independent manner via paracrine signaling from the tumor microenvironment.[16] Tumor infiltration with macrophages, which constitutively express low levels of IFNβ, can upregulate the viral-sensing genes in the tumor.[6] RNA virus infections are sensed by the melanoma differentiation-associated gene 5 (MDA5) and Retinoic acid-inducible gene I (RIGI) helicases, which signal via Mitochondrial antiviral-signaling protein (MAVS) on the mitochondrial membrane to induce expression of IFNβ.[17,18] IFNβ signals locally to induce the expression of numerous IFN-stimulated genes (ISGs), which restrict viral infection, replication, and assembly through numerous mechanisms, including the acceleration of viral genome degradation, suppression of host and viral protein translation, and interference with the assembly and release of progeny viruses.[19,20] In support of preclinical observations, IFN-responsive tumors also appear to be less likely to respond to oncolytic viruses, clinically, setting a precedent for developing mechanisms to overcome this barrier.[21]

Pharmaceutical blockade of IFN signaling/ISG function using Janus kinase (JAK)/signal transducer and activator of transcription (STAT) inhibitors, histone deacetylase inhibitors, and kinase inhibitors, such as sunitinib, are all being pursued to address this issue.[22–24] However, due to the complexity and redundancy of the innate immune response, coupled with the relative paucity of drugs that can be used for this purpose, we hypothesized that unrelated OVs with natural abilities to combat various aspects of the innate immune response may prove harmonious and provide an alternative or complement to pharmacologic

Received 23 February 2020; accepted 19 June 2020;
https://doi.org/10.1016/j.omto.2020.06.017.

Correspondence: Stephen J. Russell, MD, PhD, Department of Molecular Medicine, Mayo Clinic College of Medicine, 200 1st Street S.W., Rochester, MN 55905, USA.
E-mail: sjr@mayo.edu

 © 2020 The Author(s).
This is an open access article under the CC BY-NC-ND license (http://creativecommons.org/licenses/by-nc-nd/4.0/).

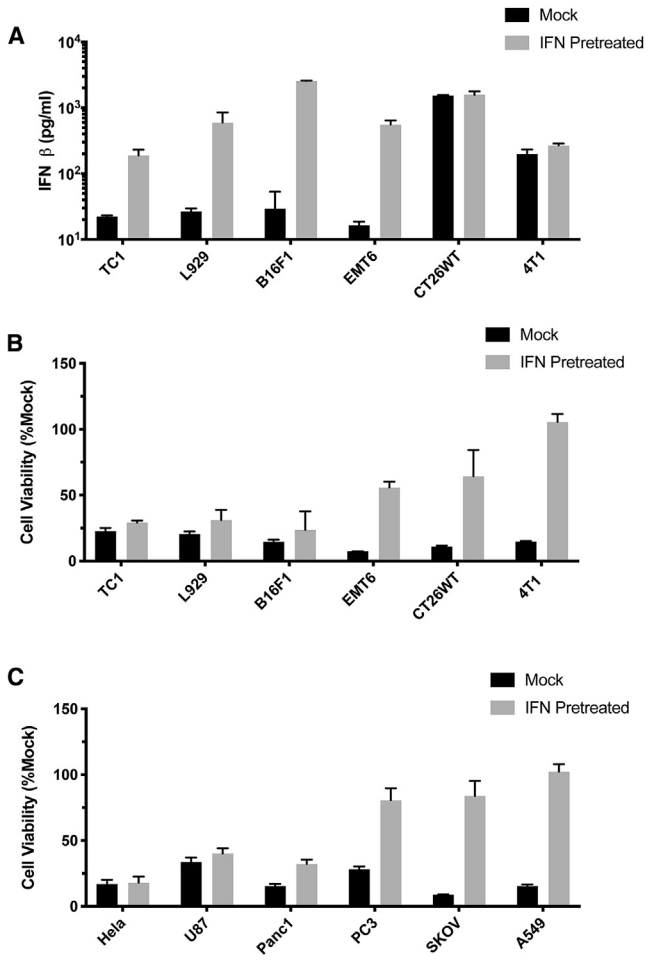

Figure 1. Heterogeneous Protective Type 1 Interferon Response in Tumor Models

(A) A panel of mouse cell lines was treated with 100 U/mL mIFNα or PBS vehicle control. Twelve hours posttreatment, cells were infected with MC_{24} at an MOI of 10. IFNβ concentration in the supernatant was quantified via ELISA at 24 h post-infection. (B and C) A panel of mouse (B) and human (C) cell lines was treated with 100 U/mL mIFNα or PBS vehicle control. Twelve hours posttreatment, cells were infected with MC_{24} at an MOI of 10. Cell viability was determined at 72 h post-infection by MTT assay. The experiments were run in triplicate, and data are represented as mean cell viability or IFN concentration ± standard deviations.

blockade.[25] With the goal of modulating as many innate defense pathways as possible through multiple mechanisms,[26] we chose to combine an oncolytic vaccinia virus (VV) with our small RNA viruses. VV, a poxvirus, has a large complex DNA genome encoding multiple innate immune combat proteins, and has been shown by Le Boeuf et al.[27] to limit innate immune restriction and restore VSV oncolysis via expression of the secreted IFN decoy receptor B18R.[27–29] VV strain Lister (VV-L) lacks expression of the B18R gene and is not directly toxic to mouse cell lines,[30] but is nevertheless able to reverse the antiviral state by blocking ISGs' effector functions, such as protein kinase R (PKR) and RNaseL, in addition to inhibiting IFN signaling via multiple mechanisms. Here, we investigated the impact of VV-L on the intratumoral replication of oncolytic MC_{24} and VSV in a model known to be resistant to all three viruses.[9,31]

RESULTS

Differential Ability of Tumor Cell Lines to Sense and Respond to Mengovirus Infection

Six murine tumor cell lines (CT26WT, 4T1, TC1, EMT6, L929, and B16F1) were infected at high MOI with MC_{24}, and supernatant concentrations of IFNβ were determined 24 h later (Figure 1A). Cell viability was measured 72 h post-infection (Figure 1B). Virus infection led to variable induction of IFNβ, but all cell lines were efficiently killed at this MOI. However, preincubation of the cells with $IFN\alpha_2$ to induce an antiviral state prior to infection led to a more uniform induction of IFNβ and, in some cases, significantly reduced MC_{24} cytotoxicity. A similar cell killing assay was conducted using a panel of human tumor cell lines infected with MC_{24} (Figure 1C), again showing generally high susceptibility of all cell lines, but significant variability in susceptibility following exposure to $IFN\alpha_2$.

Resistance to Oncolytic Virotherapy Correlates with IFN Responsiveness of CT26 Tumor Subclones

To determine whether *in vivo* resistance to oncolytic virotherapy is correlated with innate immune signaling and the induction of an antiviral state in tumor-resident cancer cells, we studied the IFN-responsive CT26WT syngeneic colon carcinoma model and its well-characterized IFN-unresponsive subclone, CT26LacZ. As shown in Figure 2A, pretreatment with 100 U/mL $IFN\alpha_2$ was completely protective in CT26WT cells against MC_{24} cytotoxicity and significantly reduced cell death in response to VSV infection. In contrast, IFN pretreatment failed to reduce viral toxicity in CT26LacZ cells, confirming the previously documented inability of this particular subclone to mount successful antiviral immunity.[15]

CT26WT and CT26LacZ cells were subsequently implanted and allowed to form tumors in the flanks of syngeneic mice, then treated with a single intratumoral injection of 1×10^8 50% tissue culture infective dose ($TCID_{50}$) of either MC_{24}NC or VSV-mIFNβ-EGFP. CT26WT tumors were essentially unresponsive to either virus therapy, and there was no survival advantage compared with the phosphate-buffered saline (PBS) treatment group (Figure 2B). In contrast, CT26LacZ-derived tumors responded to both virus therapies, resulting in significant survival advantages compared with control-treated animals (Figure 2C).

CT26WT-Derived Tumors Show Intratumoral Activation of Antiviral Gene Networks

Illlumina HiSeq RNA paired-end sequencing was used to analyze the transcriptome of *in vitro*-cultured CT26WT cells before and after a 36-h exposure to 100 U/mL $IFN\alpha_2$ and of cells isolated from a 10-day established subcutaneous CT26WT tumor (Figure 3A). A gene panel of 58 ISGs, IFN signaling genes, and inflammatory genes was based on genes with known anti-picornavirus and anti-rhabdovirus activity, and included genes with expression retained in CT26WT compared with CT26LacZ.[15,32,33] This gene panel was used to generate the heatmap in Figure 3B using average linkage and

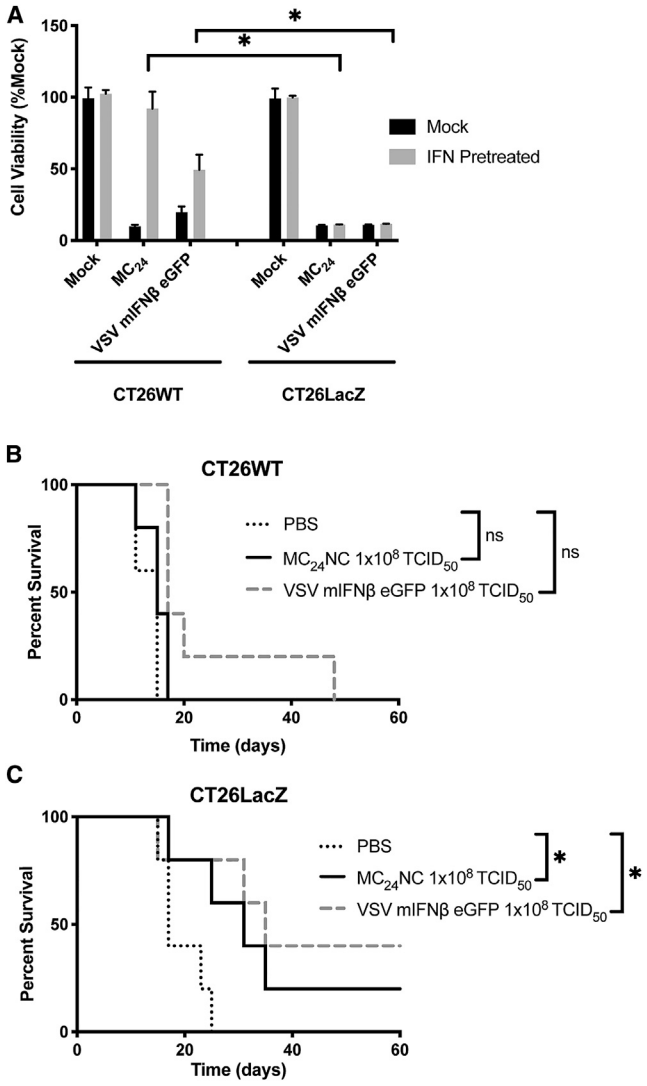

Figure 2. Interferon Responsiveness Correlates with CT26 Colon Carcinoma Susceptibility to MC_{24} and VSV *In Vitro* and *In Vivo*

CT26WT and CT26LacZ cells were treated with 100 U/mL mIFNα or PBS vehicle control. Twelve hours later, cells were infected with MC_{24} at an MOI of 10. Cell viability was determined at 72 h postinfection via MTT assay. Comparisons were based on three experimental replicates, and statistical significance was represented as follows: *$p < 0.05$. (B and C) Kaplan-Meier survival curves of mice bearing subcutaneous CT26WT (B) or CT26LacZ (C) tumors, treated with a single intratumoral (IT) injection of PBS (n = 5), 1×10^8 $TCID_{50}$ of MC_{24}NC (n = 5), or 1×10^8 $TCID_{50}$ of VSV-mIFNβ-EGFP (n = 5). Comparisons were based on log rank statistics, with $p \leq 0.05$ considered significant.

Euclidean distance. Gene expression fold change in IFN-treated CT26WT and CT26WT tumor implants was determined in relation to CT26WT cells and displayed in Figure 3C.

As anticipated, long-term IFN treatment of the CT26WT cells *in vitro* led to upregulation of numerous ISGs and IFN response factors, including IRF7, IRF9, Oasl1, Ifi44, Oas subunits, RNaseL, Eif2ak2 (PKR), and Ifih1(MDA5). Incubation with IFN also led to the downregulation of ifnb1 through negative feedback inhibition, as has been previously observed.[34] Interestingly, the tumor samples clustered strongly with the IFN-treated cells and not the untreated cells, suggesting a constitutive antiviral state was acquired after cell implantation. The CT26WT tumor showed upregulation of a number of viral-sensing genes, including Ifih1 and MAVs, and upregulation of the IFN induction and signaling intermediates IFNAR, Stat1, TLR3, and TLR7, suggesting enhanced capability to respond to oncolytic virus infection.

VV-L Is Able to Enhance the Replication and Cytotoxicity of MC_{24} and VSV-mIFNβ-EGFP after Induction of the Antiviral State

VV encodes several proteins known to interfere with induction, activation, and effector functions of IFN-mediated innate immunity.[35] Of all VV strains tested, VV-L was the least cytotoxic in our mouse cell lines and was therefore used for coinfection studies with MC_{24} or VSV (Figure S1B). Control and IFN-pretreated CT26WT cells were infected with MC_{24}, VSV, and VV-L alone, or coinfected with VV-L plus VSV or MC_{24}. Virus progeny were titrated at regular intervals (Figures 4B and 4D), and cell viability was measured 72 h postinfection (Figures 4A and 4C). VV-L had minimal impact on the viability of CT26WT cells, regardless of whether or not they had been pretreated with IFN. Also, as previously noted, both MC_{24} and VSV were highly cytotoxic in CT26WT cells, but not when the cells had been previously exposed to IFN. In contrast, when VV-L was coadministered with MC_{24} or with VSV, the cytotoxicity of these viruses in IFN-pretreated cells was fully restored. The above experiments were repeated using a human ovarian cell line, SKOV3, which was moderately sensitive to VV-L but fully susceptible to MC_{24} and VSV. SKOV3 cells became resistant to MC_{24} and VSV when pretreated with IFN. This resistance was all but eliminated following coinfection with VV-L (Figure 4E).

To determine the relative amount of VV-L required to enhance the Mengovirus infection, we infected IFN-pretreated CT26WT cells with increasing MOIs of VV-L, with or without coinfection of MC_{24} (Figure 4F). VV-L was not cytotoxic to the CT26WT cells even at the highest tested MOI. Interestingly, a VV-L MOI >1 was required to significantly increase virus cytotoxicity in MC_{24} coinfected cells, suggesting that MC_{24} and VV-L must both infect the same cell to overcome the IFN-mediated antiviral effects when the viruses are delivered concurrently.

The soluble IFN decoy receptor B18 was previously reported to enhance infection of VSV-resistant tumor cells with oncolytic VSV.[27] However, unlike other VV strains, VV-L does not express B18.[36] To confirm that the VV-L used in our studies did not contain the functional B18R gene, we isolated DNA from stocks of VV-L and VV-WR and used primers to amplify the E9L, DNA polymerase gene, and the B18 gene (Figure S1A). E9L was amplified from both stocks; however, B18 was not detected with the specific primers in the VV-L stock, further confirming the identity of the viral stocks. Interestingly, VV-WR was adapted to grow on murine cells over numerous passages and, unlike VV-L, is directly cytotoxic to CT26WT cells. As expected, we were able to show that VV-WR does enhance the cytotoxicity of MC_{24} in IFN-pretreated cells (Figure S1B).

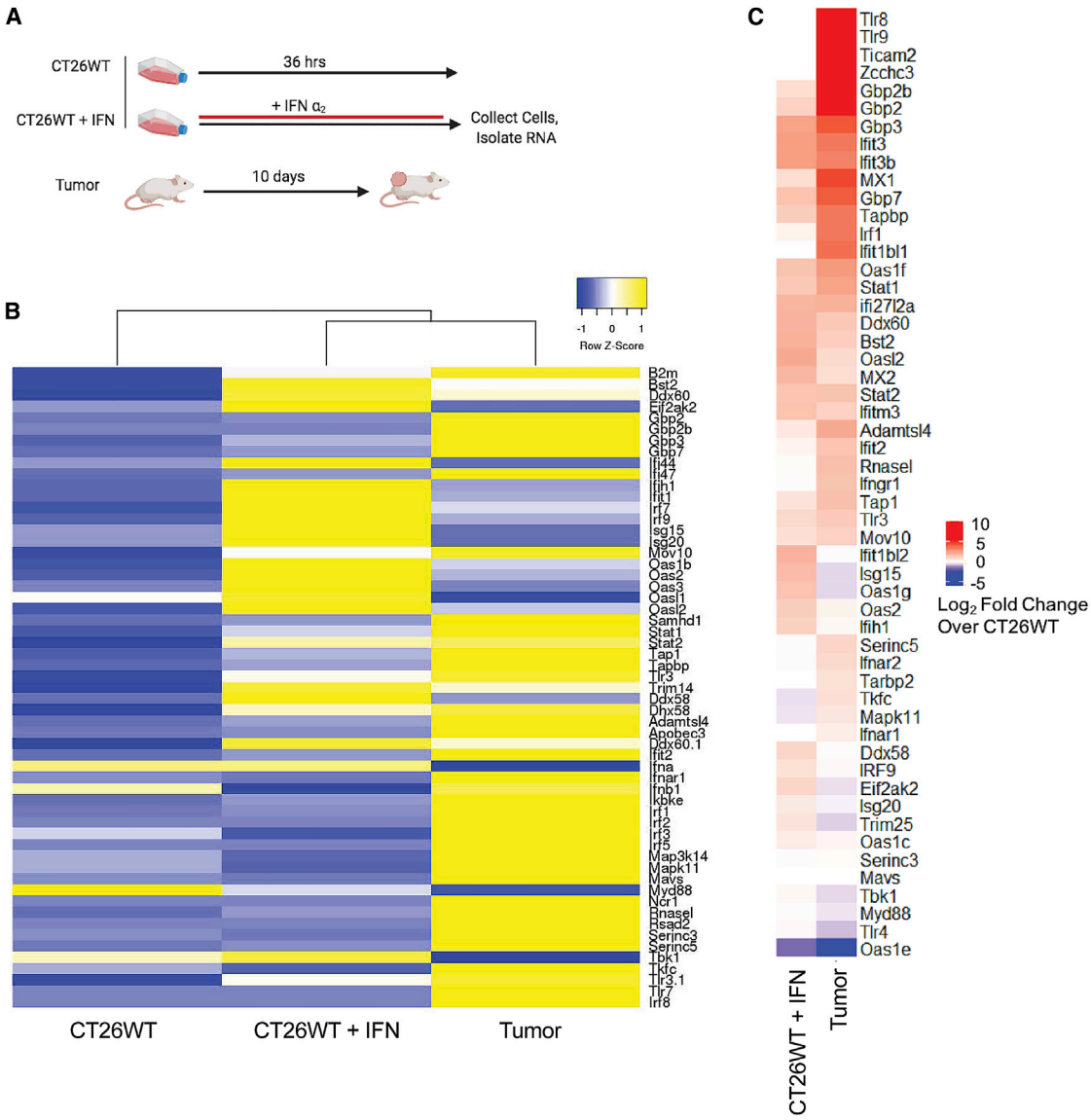

Figure 3. Genes Encoding Key Regulators of Antiviral Pathways Are Upregulated in Established Tumors

(A) Schema for whole-exome sequencing of CT26WT cells cultured with or without 100 U/mL IFNα_2 or from established tumors. RNA was isolated and sent for Illumina RNA sequencing. (B) Heatmap comparing 58 interferon-stimulated genes and inflammatory genes generated using the average FPKM of two independent samples, clustered according to average linkage and Euclidean distance. (C) Log_2(fold change) of gene expression in the 58-gene panel comparing the IFN-treated cells and tumor cells with the untreated CT26WT *in vitro*.

VV-L Enhances Intratumoral $MC_{24}NC$ Replication in CT26WT Tumors

Mice bearing CT26WT subcutaneous flank tumors received intratumoral injections of saline or VV-L daily for 2 days, followed by an intratumoral administration of $MC_{24}NC$ the next day. Tumors were excised 48 h after Mengovirus injection from six animals per group, and the unfiltered tumor lysates were subjected to $TCID_{50}$ assay on Vero cells to determine the total number of progeny virus particles (VV-L and $MC_{24}NC$). Lysates were also filtered (0.2 μm) to remove VV-L and re-titrated to quantify the filter-passing $MC_{24}NC$ particles. Quantitative PCR (qPCR) was performed to measure VV-L and $MC_{24}NC$ genomes in the tumor lysates. Analysis of the unfiltered lysates shows recovery of VV-L progeny from the majority of animals in the VV-L-only group (Figure 5C). Likewise, infectious $MC_{24}NC$ progeny were detected in the filtered tumor lysate in the single-agent $MC_{24}NC$ group. Filtration successfully removed all of the VV-L such that infectious virus was not detectable in the filtered lysate from the VV-L-only group. In the group of animals receiving combination VV-L and $MC_{24}NC$ injections, virus titers in the unfiltered and filtered tumor lysates were increased up to 100-fold compared with single-agent therapy. This was corroborated

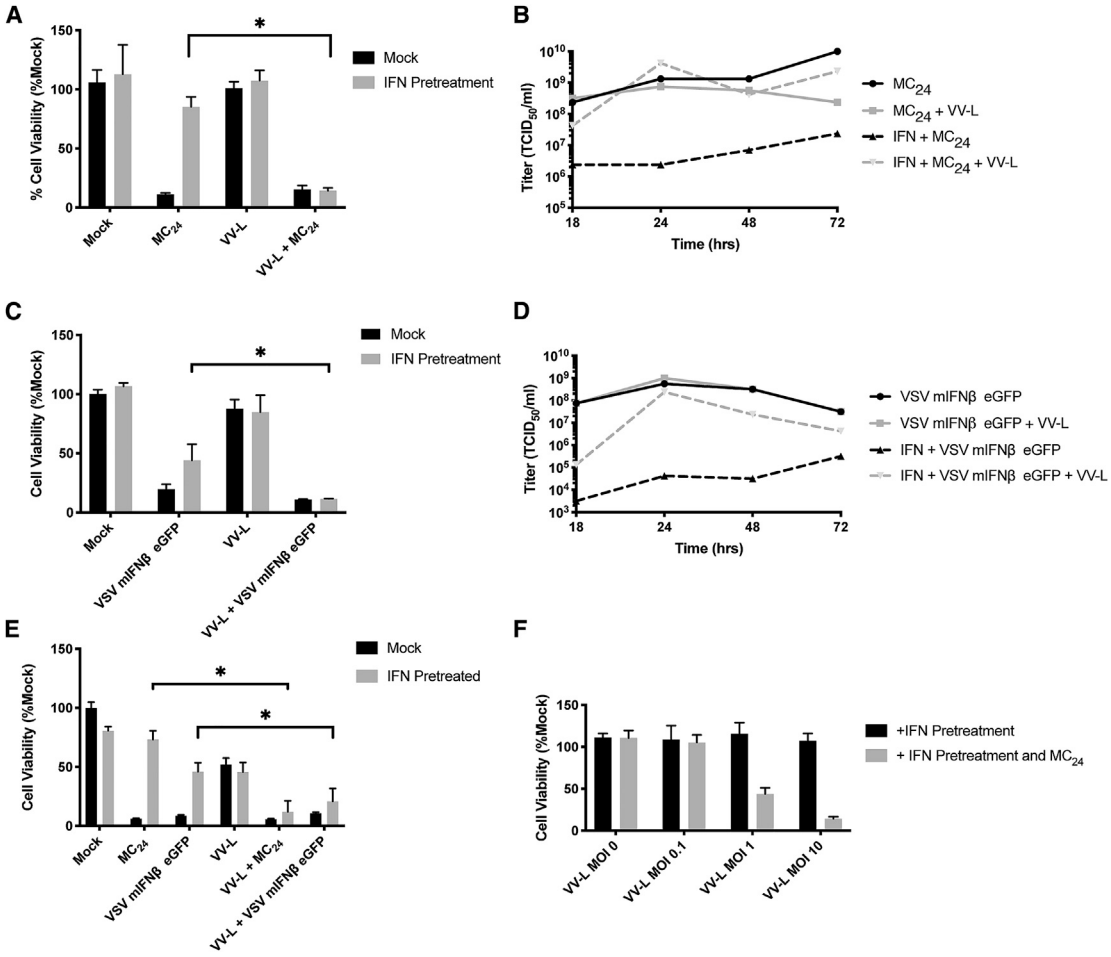

Figure 4. Vaccinia Virus Coinfection Overcomes IFN-Mediated Restraint of MC_{24} or VSV Infection *In Vitro*

Cell lines were treated with 100 U/mL mIFNα or PBS vehicle control. Twelve hours later, cells were coinfected with VV-L at an MOI of 10 and either MC_{24} (MOI 10) or VSV (MOI 1). (A, C, and E) Cell viability of CT26WT (A and C) and SKOV3 (E) cells was measured 72 h postinfection with an MTT assay. (B and D) CT26WT cell culture supernatant was collected at indicated times postinfection, passed twice through a 0.2-μm filter to remove any VV-L, and then titrated. (F) CT26WT cells pretreated with 100 U/mL mIFNα for 12 h were infected with the indicated MOI of VV-L with or without concurrent MC_{24} infection at a fixed MOI of 10. The experiments were run in triplicate, and data are represented as mean cell viability ± standard deviations or representative viral titer (*$p < 0.05$).

by the qPCR analysis of viral genome copy numbers in the tumor lysate, which showed a 100-fold increase in MC_{24}NC genomes in combination-treated mice compared with animals receiving single-agent MC_{24}NC. Although not significant, the copy number of VV-L genomes was also increased approximately 10-fold in tumor lysates from animals injected with VV-L plus MC_{24}NC compared with those receiving VV-L alone, suggesting that the MC_{24}NC may be capable of removing certain barriers to intratumoral vaccinia replication. In addition to the tumor lysates, blood samples were collected from eight animals per group on day 3 after MC_{24}NC administration, and assayed for virus genome copy numbers and infectious virus titers pre- and post-filtration through a 0.2-μm filter. In general, the MC_{24}NC and VV-L titers detected in the bloodstream were found to closely mirror those in the tumor lysates. The observed increase in intratumoral replication of MC_{24}NC was insufficient to cause a tumor regression.

VV-L Enhances the Oncolytic Efficacy of VSV-mIFNβ-EGFP in CT26WT Flank Tumors

Groups of mice bearing CT26WT subcutaneous flank tumors received a similar treatment as in Figure 5A, but with VSV-mIFNβ-EGFP in place of MC_{24}NC. Intratumoral injections of VV-L on days −2 and −1 were followed by an intratumoral injection of VSV-mIFNβ-EGFP on day 0 (n = 5 animals per group). As shown in Figure 6A, survival was significantly extended in the VV-L plus VSV-mIFNβ-EGFP combination virotherapy group compared with either of the groups that were treated with a single viral agent. In a repeat of this study, animals were euthanized, tumor lysates were harvested 72 h after VSV-mIFNβ-EGFP infection and filtered (0.2 μm) to remove VV-L progeny, and the filtered and unfiltered lysates were subjected to $TCID_{50}$ assay on Vero cells in replicates of 8. Titers of progeny VSV-mIFNβ-EGFP recovered from 0.2-μm-filtered

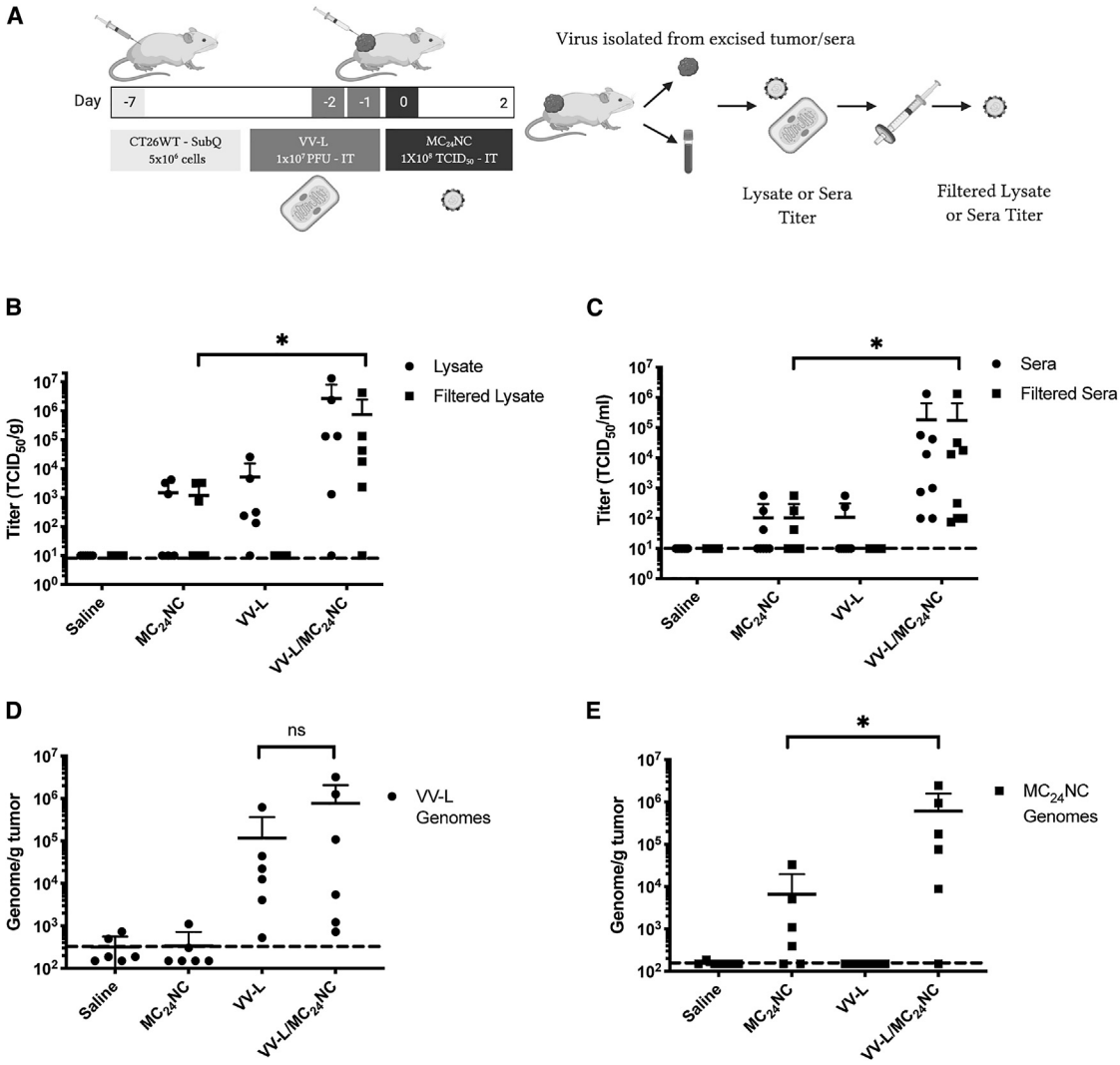

Figure 5. Vaccinia Virus Enhances Mengovirus Replication in CT26WT Tumors

Mice bearing subcutaneous CT26WT were treated according to the protocol in (A). (B) Cleared tumor lysates collected on day 2 were titrated directly or passed twice through a 0.2-μm filter to remove VV-L and then titrated to determine infectious virus titers. (C) Sera collected on day 2 were titrated directly or passed through a 0.2-μm filter twice to remove VV-L and then titrated to determine plasma viral loads. (D and E) DNA and RNA were also isolated from tumor sections, and qRT-PCR used to quantify VV-L (D) or $MC_{24}NC$ (E) genomes. Dotted lines indicate the limit of detection (*$p < 0.05$).

lysates of tumors infected with VV-L plus VSV-mIFNβ-EGFP were approximately 100-fold higher than those from tumors infected with single-agent VSV-mIFNβ-EGFP. These data indicate that VV-L is able to enhance the intratumoral amplification of VSV-mIFNβ-EGFP in the syngeneic immunocompetent CT26WT tumor model, and that this is associated with enhanced tumor response.

DISCUSSION

This study demonstrates that combining diverse oncolytic viruses can enhance antitumor efficacy by circumventing antiviral immunity. In the CT26WT model, VV-L was able to counter tumor antiviral responses, but was not sufficiently cytotoxic to directly debulk the tumor. VSV-mIFNβ-EGFP and the oncolytic Mengovirus MC_{24}, although capable of killing the tumor cells *in vitro*, replicate poorly *in vivo* in IFN-responsive tumor models, including CT26WT. Coinfection with VV-L was able to sensitize the otherwise resistant tumors to infection with both RNA viruses, enhancing the antitumor potency of VSV-mIFNβ-EGFP.

Restricted intratumoral replication of oncolytic viruses is partially attributable to the tumor and stromal cells' ability to sense the infection. The panel of human and mouse cell lines tested in this study exhibited significant heterogeneity in viral sensing and antiviral effector functions. CT26WT tumors represented the "worst-case" scenario because these cells were able to sense MC_{24} and VSV infection, as well as mount significant antiviral responses. CT26LacZ tumors, in

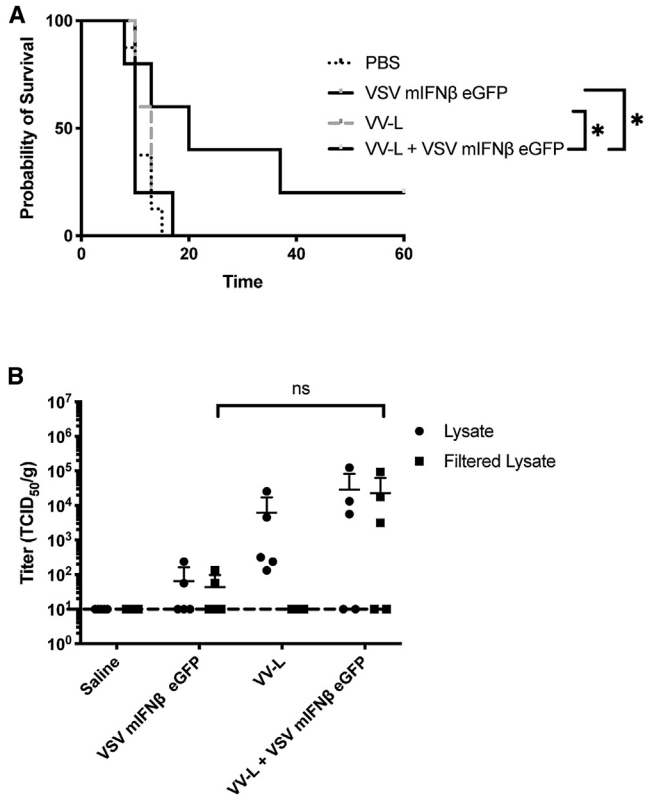

Figure 6. Vaccinia Virus Enhances VSV Replication and Therapeutic Efficacy in CT26WT Tumors

(A) Kaplan-Meier survival curve of mice bearing subcutaneous CT26WT tumors treated with VV-L on days −1 and −2 and VSV-mIFNβ-EGFP on day 0 (N = 5 animals/group). (B) Infectious virus was recovered from the tumor lysate collected on day 2 and titrated directly or passed twice through a 0.2-μm filter to remove VV-L and then titrated (*$p < 0.05$).

contrast, are able to sense infection and produce IFN, but lack the ability to respond to type 1 IFN and establish antiviral effector functions. MC_{24}NC and VSV-mIFNβ-EGFP virotherapy significantly increased overall survival in the CT26LacZ model, but their preserved ability to respond to virus infection may explain the lack of complete response. These data suggest that both virus-sensing and antiviral effector functions of tumor cells can significantly impact the efficacy of oncolytic viruses. Although CT26LacZ tumors do express a foreign and potentially immunogenic protein, beta-galactosidase, they respond very briskly to viral therapy, and tumor relapse is ultimately responsible for the death of all of the treated mice, suggesting that the initial response is not a result of adaptive antitumor immunity.

RNA transcriptome analysis of explanted CT26WT tumors revealed an inflammatory microenvironment with upregulation of ISGs known to inhibit replication of picornaviruses and rhabdoviruses. RNA was isolated from whole-tumor lysates, representing the transcriptomes of both stromal cells and tumor cells. Subcutaneous tumors grow in a poorly organized extracellular matrix occupied by malignant cells, vascular endothelial cells, stromal fibroblasts, neutrophils, macrophages, and lymphocytes.[37] Thus, antiviral and inflammatory gene transcripts could originate from stromal cells, tumor cells, or both. In CT26WT tumors, stromal cell infection and subsequent IFN production may contribute to the induction of an antiviral state. This was reported to occur in primary breast and ovarian cancer explants, where low levels of IFNβ released from stromal macrophages restricted VSV therapy.[6] In general, tumor cells account for the majority of the total cells in mouse tumor explants, suggesting a large portion of the RNA we analyzed was derived from CT26WT cells. We speculate that stromal-tumor interactions are likely activating the JAK/STAT signaling cascade in both cell types, leading to the observed constitutive expression of these antiviral genes in CT26WT tumors. The increase in antiviral gene transcripts observed in cultured CT26WT cells after they were exposed to IFN is similar to that observed in growing CT26WT tumors, providing further support for our interpretation. The conclusion from these observations is that tumors may have high basal expression of inflammatory and antiviral genes that must be countered for productive oncolytic infection.

Having established that CT26WT-derived tumors adopt an antiviral state that restricts the intratumoral spread of an oncolytic virus infection, we sought a strategy to safely sensitize these tumors and make them virus permissive. Although multiple strategies have been pursued to counter innate immune restriction, we chose to determine whether coinfection with an unrelated virus could be used to overcome this barrier. VV has long been known to rescue VSV infection in an IFN-treated cell line, partially through PKR inhibition.[38,39] VV encodes a variety of proteins known to interfere with the antiviral state at various points in the pathway. VV protein E3 masks viral double-stranded RNA (dsRNA) to prevent cellular sensing of viral infection. VV proteins A46, C6, K7, and N2 inhibit various other intermediates important for signaling of IFN induction following the sensing of virus infection. VV protein A51R stabilizes viral protein products through inhibition of ubiquitin-targeted proteasome degradation and was able to expand VSV species tropism in otherwise resistant insect cell lines.[40] JAK/STAT signal transduction downstream of the IFN receptor is inhibited by VV protein VH1. Additional VV-encoded proteins are known to inhibit ISG effector function. For example, by masking viral dsRNA, protein E3 also prevents activation of PKR and RNaseL, and protein K3 prevents PKR from halting host protein synthesis.[41] Because of the multiplicity of VV-encoded proteins known to be capable of antagonizing innate immune restrictions to virus replication, VV seemed an ideal virus to partner with our rhabdovirus and picornavirus platforms.

VV-L infection of IFN-pretreated CT26WT cells modulated the antiviral state sufficiently to restore VSV and MC_{24} replication and cytotoxicity to levels observed in untreated cells. Intratumoral replication of VSV-mIFNβ-EGFP and MC_{24}NC was significantly increased by the addition of VV-L. MC_{24}NC viremia was also significantly increased in tumors coinfected with VV-L. Higher levels of MC_{24}NC viremia offer a surrogate marker for increased intratumoral virus replication and possibly for enhanced hematogenous spread to distant sites of disease. Recovered titers of VSV-mIFNβ-EGFP and

$MC_{24}NC$ were highly variable between tumors within each experimental group, likely due to the technical limitations of intratumoral injections leading to patchy distribution of infection, coupled with the use of small tumor fragments for the virus recovery assay. The extent of $MC_{24}NC$ or VSV-mIFNβ-EGFP replication required to achieve a durable tumor response in various models remains undetermined.

In vitro experiments indicate that VV-L and the RNA virus it is paired with must coinfect the same cell in order to impact the replication of the RNA virus. We conclude that VV-L innate immune combat proteins must be expressed in the cytoplasm of a given host cell to overcome the replication barriers impacting the RNA viruses. To maximize oncolytic efficacy, VV-L must therefore localize to the same region of the tumor as VSV-mIFNβ-EGFP or $MC_{24}NC$. Individual tumor and/or stromal cells must be infected with both VV-L and an RNA virus to drive collateral lethality. Future studies will focus on the development of strategies to ensure a higher probability of both viruses infecting the same cancer cell.

Coinfection with VV-L and VSV-mIFNβ-EGFP enhanced overall survival of animals bearing CT26WT tumors, which was not observed in animals treated with the combination of VV-L and $MC_{24}NC$. This difference in therapeutic efficacy could be attributable to the IFN transgene encoded by VSV-mIFNβ-EGFP or to the difference in susceptibility of CT26WT cells to VSV versus MC_{24}. IFN-pretreated CT26WT cells were more susceptible to VSV than MC_{24}, and the mIFNβ transgene expressed from VSV may have antitumor activity. High doses of type I IFN are antiangiogenic, and low doses of IFN increase priming of adaptive immune responses.[42] Although VV-L is able to counter the antiviral functions of ISGs in infected cells, it is unlikely to interfere with the antitumor effects of released IFN (e.g., virus-encoded) on bystander cells. Addition of VV-L may therefore be the best strategy to take full advantage of the antitumor properties of IFNβ expressed from VSV, because it can counter the antiviral state induced by increasing IFN levels in the VSV-infected cells without compromising the antiangiogenic and antitumor immune-boosting properties of the IFN released from those cells. Although the primary focus of the current study has been the ability of VV-L to counter the innate immune responses of infected cells, future studies will be required to study the impact of VV-L on the activation of adaptive antitumor immunity.

Targeting of oncolytic viruses to tumors is partially attributed to the diminished IFN responsiveness of tumors compared with normal tissues. Safety is an important consideration when combining oncolytic viruses with strategies that counter antiviral responses, because this could increase virus-associated toxicity. The primary toxicities associated with the use of MC_{24} as a therapeutic agent are myocarditis and encephalitis. $MC_{24}NC$ is detargeted from neural and cardiac tissue through the use of microRNA targets, an approach that is not dependent upon intact antiviral signaling. Countering the antiviral state with VV-L would not be expected to interfere with the microRNA detargeting of $MC_{24}NC$. VSV-mIFNβ-EGFP, however, is exclusively targeted via antiviral immunity through the use of IFN as a transgene. Nevertheless, virus-mediated toxicity was not observed in any of the studies reported in this manuscript using combinations of VV-L with $MC_{24}NC$ or VSV-mIFNβ-EGFP.

VV-L replication in the models used in this study was likely restricted to the virus-injected tumors with limited hematogenous spread of the virus.[43] The majority of animals did not have detectable VV-L in the serum, and those that did had peak levels of less than 10^3 $TCID_{50}$/mL, suggesting that VV-L has very limited ability to disseminate beyond the injected tumor. Although toxicities to normal tissues as a consequence of combining VV-L with RNA viruses was not observed in the studies reported here, there are several effective antiviral agents that could be administered to limit VV-L replication if toxicity were ever observed.[44] These anti-poxvirus agents provide an additional layer of safety for clinical translation of VV-L in combination with other oncolytic agents.

A combination of VV-L-encoded immune combat proteins likely synergize to remove multiple antiviral barriers to RNA viruses. Due to the number and diverse activities of VV-L-encoded proteins, it is difficult to isolate a single protein function capable of reversing the antiviral state in CT26WT tumors. Of note, previous reports have stated that non-Lister strains of VV can enhance the antitumor activity of VSV because of the actions of B18, a soluble VV-encoded IFN decoy receptor.[27] However, VV-L does not express B18.[36] Furthermore, the IFN scavenging action of B18 can only prevent induction of the antiviral state and did not immediately reverse the antiviral state as we have observed in our studies with VV-L. VV strains lacking a functional IFN decoy receptor were associated with lower frequencies of neurological complications when used as smallpox vaccines, suggesting that VV-L may have a superior safety profile compared with other VV strains as a companion for oncolytic RNA virus therapy.[45]

To summarize, VV infection of a tumor can transiently reverse an intratumoral antiviral state leading to enhanced propagation and antitumor activity of oncolytic picornaviruses and/or rhabdoviruses. Our study demonstrates that combining diverse viral vectors may be a highly promising approach to overcome one of the most significant barriers to the success of single-agent oncolytic virotherapy.

MATERIALS AND METHODS

Cell Lines

CT26WT (CRL-2638; American Type Culture Collection [ATCC]), CT26LacZ (CRL-2639; ATCC), TC-1 (provided by T.C. Wu of Johns Hopkins University), and 4T1 (CRL-2538; ATCC) were maintained in RPMI 1640 medium (Thermo Scientific, MA, USA) supplemented with 10% fetal bovine sera (FBSs). L929 (CCL-1; ATCC), B16-F1 (CRL-6323; ATCC), Vero (CCL-81; ATCC), HeLa (CCL-2; ATCC), U-87 MG (HTB-14; ATCC), PANC-1 (CRL-146; ATCC), and A549 (CCL-185; ATCC) were maintained in DMEM (Thermo Scientific, MA, USA) supplemented with 10% FBS. SKOV3 (HTB-77; ATCC) cell lines were grown in McCoy's 5a medium (30-2007; ATCC)

supplemented with 10% FBS. PC3 (CCL-2; ATCC) cell lines were maintained in F12K media (30-2004; ATCC) supplemented with 10% FBS. EMT-6 (CRL-2755; ATCC) cell lines were maintained in Weymouth's media (MD-7193; ATCC) supplemented with 15% FBS. Cell lines were purchased from and verified by the ATCC (Manassas, VA, USA). All media were supplemented with 100 U/mL penicillin and 100 μg/mL streptomycin, and cells were incubated in a humidified 37°C incubator with 5% CO_2.

Propagation and Titration of Viruses

VSV-mIFNβ-EGFP, MC_{24}, and MC_{24}NC were rescued as previously described.[8,46] VV-L was obtained from ATCC (VR-1549). VSV-mIFNβ-EGFP and VV-L were amplified on Vero cells. MC_{24} and MC_{24}NC were rescued and amplified on HeLa cells. Viral stocks were tested for sterility and endotoxin contamination prior to use in animals. Vero cells in 96-well plates were used for calculation of $TCID_{50}$ using the Spearman-Karber equation, and Vero cells in six-well plates were used to calculate plaque-forming units as previously described.[47]

Amplification of E9L and B18 Genes from VV

The primers 5′-AAGCTTATGGATGTTCGGTGC-3′ and 5′-GAGCTCTTATGCTTCGTAAAAT-3′ were used to amplify the E9L gene region in VV. The primers 5′-GTCGTCTGATTTATG TTTTAAATATC-3′ and 5′-TACTCGAGTCATACTTTG-3′ were used to amplify the B18 gene region in VV.

Cell Viability Assays

The cells were plated at a density of 10^4 cells/well in 96-well plates. The cells were incubated with 100 U/mL species-specific IFNα (752804 and 592704; BioLegend) for 12 h and then infected with the indicated MOI of virus or virus combination for 2 h in Opti-MEM media and washed twice with PBS, and then normal growth medium was added. The cells were assayed for proliferation at 72 h postinfection with 3-(4, 5-dimethylthiazolyl-2)-2, 5 diphenyltetrazolium bromide (30-1010K; ATCC) according to the manufacturer's protocols.

IFN ELISA

Murine IFNβ ELISAs were purchased (42400; PBL Assay Science) and used to quantify the concentration of mIFNβ in cellular supernatants. A total of 5×10^4 CT26WT cells were plated in 24-well plates and incubated for 2 h with MC_{24} at an MOI of 10. Cell culture supernatants were collected 24 h after virus infection and assayed following the manufacturer's instructions.

Mice and Tumor Models

Mayo Clinic Institutional Animal Care and Use Committee approved all animal studies. Six-week-old BALB/c mice were purchased from Jackson Laboratories. A total of 5×10^6 washed CT26WT or CT26LacZ cells were implanted subcutaneously in the right flank. Viruses were diluted to the indicated dose in PBS and injected intratumorally.

All tumor-bearing mice were observed daily. Mice were weighed and tumor size was measured three times per week. Handheld calipers were used to measure tumor volume. Blood was obtained through cardiac puncture at the time of euthanasia. Harvested tissues were immediately sectioned into a vessel and flash frozen.

Tissue Processing

Virus recovery was conducted from frozen tumor samples that were weighed and homogenized in 3 vol (w/v) of Opti-MEM buffer; the supernatant was clarified by centrifugation at $12{,}000 \times g$ for 10 min. The tumor lysate was diluted 10× and used for $TCID_{50}$ assays. RNA and DNA were isolated from frozen tumor samples using commercially available kits. Total RNA was isolated from frozen tissue sections using an RNeasy Plus Universal mini kit (73404; QIAGEN) according to the manufacturer's instructions. Tumor DNA was isolated from frozen tissue sections using a DNeasy Blood and Tissue kit (69054; QIAGEN) according to the manufacturer's instructions.

Quantitative reverse transcription PCR for MC_{24}NC viral genomes was conducted using the RNA isolated from the tumor samples. Primer pair 5′-CCTGGTCCTGTCTTCTTG-3′ and 5′-GCA AAGGGTCGCTACAG-3′ was used to amplify a conserved region in the 5′ noncoding region of MC_{24}NC, and probe 5′-AAG CAGTTCCTCTGGACGCTTC-3′ was used with the TaqMan RNA to C_t kit (439265; Applied Biosystems) to detect the amplification according to the manufacturer's protocol. *In vitro*-transcribed MC_{24}NC genomic RNA was prepared using a MEGAscript T7 Transcription kit (AM1334; Thermo Fisher Scientific), purified with a MEGAscript Transcription Clean-Up kit (AM1908; Thermo Fisher Scientific), and used to generate a standard curve for genomic quantification.

qPCR for VV-L viral genomes was conducted using the RNA isolated from the tumor samples. Primer pair 5′-AAGCTTATGGAT GTTCGGTGC-3′ and 5′-GAGCTCTTATGCTTCGTAAAAT-3′ was used to amplify the VV E9L open reading frame (ORF) and clone into pcDNA3.1 for use as a standard curve. A TaqManMinor Groove Binding (MGB) probe (Applied Biosystems) with the sequence 5′-AGGACGTAGAATGATCTTGTA-3′ was used to amplify and detect a region in VV E9L polymerase with TaqMan Universal PCR master mix (4364338; Applied Biosystem) as previously described.[48]

RNA Sequencing

CT26WT cells were seeded at a density of 5×10^5 cells/well in a six-well plate and allowed to adhere for 12 h. 100 U/mL species-specific IFNα was added to two wells, and the cells were incubated for an additional 30 h. The cells were trypsinized, washed twice with PBS, and collected for freezing via centrifugation at $0.2 \times g$ for 10 min. Six-week-old BALB/c mice were purchased from Jackson Laboratories (n = 2) and subcutaneously injected with 5×10^6 washed CT26WT cells in the right flank. The tumors were allowed to grow for 10 days, at which point the mice were euthanized and the tumors were excised and flash frozen. RNA was extracted from frozen cells or tumor sections using the RNeasy Plus Universal mini kit (73404; QIAGEN).

Polyadenylated RNA was isolated with NEBNext Ultra II (E7103; NEB) and sequenced on Illumina 2×150 paired-end sequencing to generate 40M paired-end reads per sample. Paired ends were aligned, trimmed, and mapped to mouse BALB/cJ (BALB_cJ_v1/Ensembl release 95) reference genome using STAR.[49] BAM file reads were counted using the R package GenomicAlignments, and DESeq2 was used to obtain normalized counts and fold change.[50,51] Heatmaps were created using the R package Complex Heatmap for fold change.[52] AIR: RNA-Seq data analysis software (Sequentia Biotech, Barcelona, Spain) was used to generate differential gene expression analysis based on the negative binomial distribution to generate fragments per kilobase of transcript per million mapped reads (FPKM) for each condition as previously described.[53] The heatmapper software package was used to cluster the conditions based on the average linkage and Euclidean distance of 58 IFN signaling intermediates, ISGs, and other immune-regulatory genes.[54]

Statistical Analysis

GraphPad Prism (San Diego, CA, USA) was used to assess the results for statistical significance. IFN production, cell viability assays, genomic copy numbers, and viral titers were analyzed initially with an ANOVA on ranks, and if significance was reached, a specific paired two-tailed t test was used to complete the analysis. Kaplan-Meier curve and the Mantel-Cox log rank test were used to determine the significance of survival studies.

Data Availability

Data are available from the corresponding author upon reasonable request.

SUPPLEMENTAL INFORMATION

Supplemental Information can be found online at https://doi.org/10.1016/j.omto.2020.06.017.

AUTHOR CONTRIBUTIONS

J.W.M., A.J.S., and S.J.R. conceived the project. J.W.M. and V.P. performed *in vitro* experiments. J.W.M. performed *in vivo* experiments. J.W.M. and T.M.W. performed the RNA sequencing analysis. J.W.M., A.J.S., and S.J.R. wrote the manuscript. A.J.S. and S.J.R. supervised the project.

CONFLICTS OF INTEREST

S.J.R. is chief executive officer at Vyriad, an oncolytic virus company. S.J.R. and Mayo Clinic hold equity in Vyriad.

ACKNOWLEDGMENTS

The authors thank Rebecca A. Nace, veterinary technologist (Mayo Clinic), for her invaluable technical assistance and expertise with small-animal experiments. We also thank Ann C. Palmenberg of the University of Wisconsin for the kind gifts of the pF/R-wt and Rz-pMwt plasmids and communications regarding their use. We also thank T.C. Wu of Johns Hopkins University, Department of Gynecologic Pathology for the kind gift of the TC-1 cell line. The authors also respect and acknowledge the contribution of Henrietta Lacks and HeLa cells to biomedical research. J.W.M. and T.M.W. were supported by the Medical Scientist Training Program at the Mayo Clinic Alix School of Medicine, and this work was funded by Al and Mary Agnes McQuinn and Mayo Clinic.

REFERENCES

1. Stojdl, D.F., Lichty, B., Knowles, S., Marius, R., Atkins, H., Sonenberg, N., and Bell, J.C. (2000). Exploiting tumor-specific defects in the interferon pathway with a previously unknown oncolytic virus. Nat. Med. *6*, 821–825.
2. Lawler, S.E., Speranza, M.C., Cho, C.F., and Chiocca, E.A. (2017). Oncolytic Viruses in Cancer Treatment: A Review. JAMA Oncol. *3*, 841–849.
3. Balachandran, S., and Barber, G.N. (2000). Vesicular stomatitis virus (VSV) therapy of tumors. IUBMB Life *50*, 135–138.
4. Maroun, J., Muñoz-Alía, M., Ammayappan, A., Schulze, A., Peng, K.W., and Russell, S. (2017). Designing and building oncolytic viruses. Future Virol. *12*, 193–213.
5. Kurokawa, C., and Galanis, E. (2019). Interferon signaling predicts response to oncolytic virotherapy. Oncotarget *10*, 1544–1545.
6. Liu, Y.P., Suksanpaisan, L., Steele, M.B., Russell, S.J., and Peng, K.W. (2013). Induction of antiviral genes by the tumor microenvironment confers resistance to virotherapy. Sci. Rep. *3*, 2375.
7. Zhang, L., Steele, M.B., Jenks, N., Grell, J., Suksanpaisan, L., Naik, S., Federspiel, M.J., Lacy, M.Q., Russell, S.J., and Peng, K.W. (2016). Safety Studies in Tumor and Non-Tumor-Bearing Mice in Support of Clinical Trials Using Oncolytic VSV-IFNβ-NIS. Hum. Gene Ther. Clin. Dev. *27*, 111–122.
8. Ruiz, A.J., Hadac, E.M., Nace, R.A., and Russell, S.J. (2016). MicroRNA-Detargeted Mengovirus for Oncolytic Virotherapy. J. Virol. *90*, 4078–4092.
9. Shors, S.T., Beattie, E., Paoletti, E., Tartaglia, J., and Jacobs, B.L. (1998). Role of the vaccinia virus E3L and K3L gene products in rescue of VSV and EMCV from the effects of IFN-alpha. J. Interferon Cytokine Res. *18*, 721–729.
10. Ruiz, A.J., and Russell, S.J. (2015). MicroRNAs and oncolytic viruses. Curr. Opin. Virol. *13*, 40–48.
11. Felt, S.A., and Grdzelishvili, V.Z. (2017). Recent advances in vesicular stomatitis virus-based oncolytic virotherapy: a 5-year update. J. Gen. Virol. *98*, 2895–2911.
12. Barber, G.N. (2005). VSV-tumor selective replication and protein translation. Oncogene *24*, 7710–7719.
13. Naik, S., Nace, R., Barber, G.N., and Russell, S.J. (2012). Potent systemic therapy of multiple myeloma utilizing oncolytic vesicular stomatitis virus coding for interferon-β. Cancer Gene Ther. *19*, 443–450.
14. Moerdyk-Schauwecker, M., Shah, N.R., Murphy, A.M., Hastie, E., Mukherjee, P., and Grdzelishvili, V.Z. (2013). Resistance of pancreatic cancer cells to oncolytic vesicular stomatitis virus: role of type I interferon signaling. Virology *436*, 221–234.
15. Ruotsalainen, J.J., Kaikkonen, M.U., Niittykoski, M., Martikainen, M.W., Lemay, C.G., Cox, J., De Silva, N.S., Kus, A., Falls, T.J., Diallo, J.S., et al. (2015). Clonal variation in interferon response determines the outcome of oncolytic virotherapy in mouse CT26 colon carcinoma model. Gene Ther. *22*, 65–75.
16. Barber, G.N. (2001). Host defense, viruses and apoptosis. Cell Death Differ. *8*, 113–126.
17. Feng, Q., Hato, S.V., Langereis, M.A., Zoll, J., Virgen-Slane, R., Peisley, A., Hur, S., Semler, B.L., van Rij, R.P., and van Kuppeveld, F.J. (2012). MDA5 detects the double-stranded RNA replicative form in picornavirus-infected cells. Cell Rep. *2*, 1187–1196.
18. Barral, P.M., Sarkar, D., Su, Z.Z., Barber, G.N., DeSalle, R., Racaniello, V.R., and Fisher, P.B. (2009). Functions of the cytoplasmic RNA sensors RIG-I and MDA-5: key regulators of innate immunity. Pharmacol. Ther. *124*, 219–234.
19. Stojdl, D.F., Abraham, N., Knowles, S., Marius, R., Brasey, A., Lichty, B.D., Brown, E.G., Sonenberg, N., and Bell, J.C. (2000). The murine double-stranded RNA-dependent protein kinase PKR is required for resistance to vesicular stomatitis virus. J. Virol. *74*, 9580–9585.
20. Silverman, R.H. (2007). Viral encounters with 2′,5′-oligoadenylate synthetase and RNase L during the interferon antiviral response. J. Virol. *81*, 12720–12729.

21. Kurokawa, C., Iankov, I.D., Anderson, S.K., Aderca, I., Leontovich, A.A., Maurer, M.J., Oberg, A.L., Schroeder, M.A., Giannini, C., Greiner, S.M., et al. (2018). Constitutive Interferon Pathway Activation in Tumors as an Efficacy Determinant Following Oncolytic Virotherapy. J. Natl. Cancer Inst. *110*, 1123–1132.

22. Escobar-Zarate, D., Liu, Y.P., Suksanpaisan, L., Russell, S.J., and Peng, K.W. (2013). Overcoming cancer cell resistance to VSV oncolysis with JAK1/2 inhibitors. Cancer Gene Ther. *20*, 582–589.

23. Fox, C.R., and Parks, G.D. (2019). Histone Deacetylase Inhibitors Enhance Cell Killing and Block Interferon-Beta Synthesis Elicited by Infection with an Oncolytic Parainfluenza Virus. Viruses *11*, 431.

24. Jha, B.K., Dong, B., Nguyen, C.T., Polyakova, I., and Silverman, R.H. (2013). Suppression of antiviral innate immunity by sunitinib enhances oncolytic virotherapy. Mol. Ther. *21*, 1749–1757.

25. Muller, F.L., Aquilanti, E.A., and DePinho, R.A. (2015). Collateral Lethality: A new therapeutic strategy in oncology. Trends Cancer *1*, 161–173.

26. Wong, S.T., and Goodin, S. (2009). Overcoming drug resistance in patients with metastatic breast cancer. Pharmacotherapy *29*, 954–965.

27. Le Boeuf, F., Diallo, J.S., McCart, J.A., Thorne, S., Falls, T., Stanford, M., Kanji, F., Auer, R., Brown, C.W., Lichty, B.D., et al. (2010). Synergistic interaction between oncolytic viruses augments tumor killing. Mol. Ther. *18*, 888–895.

28. Alcamí, A., Symons, J.A., and Smith, G.L. (2000). The vaccinia virus soluble alpha/beta interferon (IFN) receptor binds to the cell surface and protects cells from the antiviral effects of IFN. J. Virol. *74*, 11230–11239.

29. Colamonici, O.R., Domanski, P., Sweitzer, S.M., Larner, A., and Buller, R.M. (1995). Vaccinia virus B18R gene encodes a type I interferon-binding protein that blocks interferon alpha transmembrane signaling. J. Biol. Chem. *270*, 15974–15978.

30. Hughes, J., Wang, P., Alusi, G., Shi, H., Chu, Y., Wang, J., Bhakta, V., McNeish, I., McCart, A., Lemoine, N.R., and Wang, Y. (2015). Lister strain vaccinia virus with thymidine kinase gene deletion is a tractable platform for development of a new generation of oncolytic virus. Gene Ther. *22*, 476–484.

31. Paez, E., and Esteban, M. (1984). Resistance of vaccinia virus to interferon is related to an interference phenomenon between the virus and the interferon system. Virology *134*, 12–28.

32. Kumar, R., Choubey, D., Lengyel, P., and Sen, G.C. (1988). Studies on the role of the 2′-5′-oligoadenylate synthetase-RNase L pathway in beta interferon-mediated inhibition of encephalomyocarditis virus replication. J. Virol. *62*, 3175–3181.

33. Liu, S.Y., Sanchez, D.J., Aliyari, R., Lu, S., and Cheng, G. (2012). Systematic identification of type I and type II interferon-induced antiviral factors. Proc. Natl. Acad. Sci. USA *109*, 4239–4244.

34. Li, Y., Li, C., Xue, P., Zhong, B., Mao, A.P., Ran, Y., Chen, H., Wang, Y.Y., Yang, F., and Shu, H.B. (2009). ISG56 is a negative-feedback regulator of virus-triggered signaling and cellular antiviral response. Proc. Natl. Acad. Sci. USA *106*, 7945–7950.

35. Smith, G.L., Benfield, C.T.O., Maluquer de Motes, C., Mazzon, M., Ember, S.W.J., Ferguson, B.J., and Sumner, R.P. (2013). Vaccinia virus immune evasion: mechanisms, virulence and immunogenicity. J. Gen. Virol. *94*, 2367–2392.

36. Smith, G.L., and Chan, Y.S. (1991). Two vaccinia virus proteins structurally related to the interleukin-1 receptor and the immunoglobulin superfamily. J. Gen. Virol. *72*, 511–518.

37. Vähä-Koskela, M., and Hinkkanen, A. (2014). Tumor Restrictions to Oncolytic Virus. Biomedicines *2*, 163–194.

38. Thacore, H.R., and Youngner, J.S. (1973). Rescue of vesicular stomatitis virus from interferon-induced resistance by superinfection with vaccinia virus. II. Effect of UV-inactivated vaccinia and metabolic inhibitors. Virology *56*, 512–522.

39. Whitaker-Dowling, P., and Youngner, J.S. (1983). Vaccinia rescue of VSV from interferon-induced resistance: reversal of translation block and inhibition of protein kinase activity. Virology *131*, 128–136.

40. Gammon, D.B., Duraffour, S., Rozelle, D.K., Hehnly, H., Sharma, R., Sparks, M.E., West, C.C., Chen, Y., Moresco, J.J., Andrei, G., et al. (2014). A single vertebrate DNA virus protein disarms invertebrate immunity to RNA virus infection. eLife *3*, e02910.

41. Smith, G.L., Talbot-Cooper, C., and Lu, Y. (2018). How Does Vaccinia Virus Interfere With Interferon? Adv. Virus Res. *100*, 355–378.

42. Gajewski, T.F., and Corrales, L. (2015). New perspectives on type I IFNs in cancer. Cytokine Growth Factor Rev. *26*, 175–178.

43. Zonov, E., Kochneva, G., Yunusova, A., Grazhdantseva, A., Richter, V., and Ryabchikova, E. (2016). Features of the Antitumor Effect of Vaccinia Virus Lister Strain. Viruses *8*, 20.

44. Chan, W.M., and McFadden, G. (2014). Oncolytic Poxviruses. Annu. Rev. Virol. *1*, 119–141.

45. Symons, J.A., Alcamí, A., and Smith, G.L. (1995). Vaccinia virus encodes a soluble type I interferon receptor of novel structure and broad species specificity. Cell *81*, 551–560.

46. Naik, S., Nace, R., Federspiel, M.J., Barber, G.N., Peng, K.W., and Russell, S.J. (2012). Curative one-shot systemic virotherapy in murine myeloma. Leukemia *26*, 1870–1878.

47. Cotter, C.A., Earl, P.L., Wyatt, L.S., and Moss, B. (2015). Preparation of cell cultures and vaccinia virus stocks. Curr. Protoc. Microbiol. *39*, 14A.3.1–14A.3.18.

48. Baker, J.L., and Ward, B.M. (2014). Development and comparison of a quantitative TaqMan-MGB real-time PCR assay to three other methods of quantifying vaccinia virions. J. Virol. Methods *196*, 126–132.

49. Dobin, A., Davis, C.A., Schlesinger, F., Drenkow, J., Zaleski, C., Jha, S., Batut, P., Chaisson, M., and Gingeras, T.R. (2013). STAR: ultrafast universal RNA-seq aligner. Bioinformatics *29*, 15–21.

50. Lawrence, M., Huber, W., Pagès, H., Aboyoun, P., Carlson, M., Gentleman, R., Morgan, M.T., and Carey, V.J. (2013). Software for computing and annotating genomic ranges. PLoS Comput. Biol. *9*, e1003118.

51. Love, M.I., Huber, W., and Anders, S. (2014). Moderated estimation of fold change and dispersion for RNA-seq data with DESeq2. Genome Biol. *15*, 550.

52. Gu, Z., Eils, R., and Schlesner, M. (2016). Complex heatmaps reveal patterns and correlations in multidimensional genomic data. Bioinformatics *32*, 2847–2849.

53. Vara, C., Paytuví-Gallart, A., Cuartero, Y., Le Dily, F., Garcia, F., Salvà-Castro, J., Gómez-H, L., Julià, E., Moutinho, C., Aiese Cigliano, R., et al. (2019). Three-dimensional genomic structure and cohesin occupancy correlate with transcriptional activity during spermatogenesis. Cell Rep. *28*, 352–367.e9.

54. Babicki, S., Arndt, D., Marcu, A., Liang, Y., Grant, J.R., Maciejewski, A., and Wishart, D.S. (2016). Heatmapper: web-enabled heat mapping for all. Nucleic Acids Res. *44* (W1), W147–W153.